Identification and functional characterization of the candidate tumor suppressor gene TRIT1 in human lung cancer

Monica Spinola[1], Antonella Galvan[1], Carmen Pignatiello[1], Barbara Conti[2], Ugo Pastorino[2], Bjorn Nicander[3], Rita Paroni[4] and Tommaso A Dragani*,[1]

[1]*Department of Experimental Oncology and Laboratories, Istituto Nazionale Tumori, Via G. Venezian 1, 20133 Milan, Italy;* [2]*Department of Thoracic Surgery, Istituto Nazionale Tumori, Milan, Italy;* [3]*Department of Plant Biology, Swedish University of Agricultural Sciences, Uppsala, Sweden;* [4]*Department of Medicine, Surgery and Dental Sciences, University of Milan, San Paolo Hospital, Milan, Italy*

tRNA-isopentenyltransferase (tRNA-IPT) catalyses the addition of N^6-isopentenyladenosine (i^{6}A) on residue 37 of tRNA molecules that bind codons starting with uridine. Post-transcriptional modifications of tRNA molecules have been demonstrated to be essential in maintaining the correct reading frame of the translational machinery, thus improving fidelity and efficiency of protein synthesis. We show here that the human tRNA-isopentenyltransferase (TRIT1) gene encodes a complex pattern of mRNA variants through alternative splicing in both normal and tumor lung tissue and that the nonsense suppressor activity of tRNA-IPT is maintained only in the full-length mRNA isoform, as revealed by gene complementation in yeast. Expression of the full-length transcript was downregulated 6–14-fold in lung adenocarcinomas as compared to normal lung tissue. A549 lung cancer cells transfected to express the functional TRIT1 gene formed significantly smaller colonies with reduced scattering on the edges and had only limited ability to induce tumors in nude mice. Our findings raise the possibility of TRIT1 as a candidate lung tumor suppressor.

Introduction

Isopentenyltransferases (IPTs) are a family of enzymes, conserved from microorganisms to mammals, that catalyse the biosynthesis of cytokinins in both a tRNA-bound and a tRNA-free form through addition of adenine to either tRNA (tRNA-IPTs, EC 2.5.1.8) or AMP (cytokinin synthases, EC 2.5.1.27) acceptor

molecules (Takei *et al.*, 2001). tRNA-free cytokinins are present in plants where they act as phytohormones to promote and regulate several growth and developmental processes (Miller *et al.*, 1955; Mok, 1994). Cytokinins in their tRNA-bound form are found in several organisms, including mammals (Persson *et al.*, 1994) and represent one of the numerous post-transcriptional modifications of tRNA molecules. At present, 81 different modified residues have been identified that most frequently involve the wobble position (residue 34) and the position 3′ adjacent to the anticodon (residue 37) (Rozenski *et al.*, 1999). All of these modifications have been shown to be essential in maintaining the correct reading frame of the translational machinery, thus improving fidelity and efficiency of protein synthesis and avoiding errors that could be detrimental for cells (Persson, 1993; Bjork *et al.*, 1999; Urbonavicius *et al.*, 2001).

N^6-isopentenyladenosine (i^{6}A) is the only known cytokinin existing in animal tRNAs and is specifically found at position 37 of tRNA molecules that bind codons starting with uridine (Persson *et al.*, 1994). Addition of i^{6}A on residue 37 of tRNA molecules is catalysed by tRNA-IPTs using △2-dimethylallyl pyrophosphate as donor of the isopentenyl group. tRNA-IPT genes have been identified and cloned in several organisms, including *miaA* from *Escherichia coli* (Caillet and Droogmans, 1988), *MOD5* from *Saccharomyces cerevisiae* (Dihanich *et al.*, 1987), TRIT1 from *Homo sapiens* (Golovko *et al.*, 2000), *gro-1* from *Caenorhabditis elegans* (Lemieux *et al.*, 2001), and *AtIPT2* from *Arabidopsis thaliana* (Takei *et al.*, 2001). Mutations in tRNA-IPT genes significantly influence several biological functions: mutations in the *miaA* gene affect bacterial growth rate (Diaz *et al.*, 1987) and the rate of GC to TA spontaneous transversions (Connolly and Winkler, 1989); yeast strains with defective MOD5 activity suppress nonsense mutations less efficiently; and *gro-1* mutants of *C. elegans* show a slower developmental rate and an increased lifespan.

Deregulation of translation has been associated with malignant characteristics and cancer induction (Bjornsti and Houghton, 2004). Post-transcriptional modifications of tRNAs are important in assuring correct

protein synthesis and alterations in tRNA modifications have been related to the cancer phenotype (Dirheimer et al., 1995). In the present study, we compared TRIT1 expression in normal lung parenchyma and lung tumors, and analysed cancer cell lines overexpressing the biochemically functional TRIT1 variant. Our results identify the TRIT1 gene as a potential negative regulator of lung carcinogenesis.
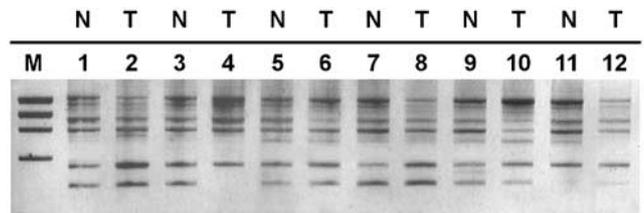
Results

TRIT1 gene expression in human lung

To explain unsuccessful attempts to amplify the TRIT1 gene from human lung cDNAs using primers including the start and stop codon of clone AF074918 isolated from embryo (Golovko et al., 2000), we screened a human lung cDNA library for possible differences in the sequence of the TRIT1 gene. PCR screening revealed nine positive clones, six of which were confirmed by direct sequencing to contain the TRIT1 gene. Sequence analysis showed that the 5′-end of all clones lacked the start codon reported in sequence AF074918 but contained another putative ATG start codon in exon 1 corresponding to nucleotide 183. Since this putative start codon is in-frame with the reported start signal, the protein product of the clones we found (411 amino acids) is identical to the product of the annotated sequence but lacks the initial 56 residues.

We analysed TRIT1 expression in human lung cDNAs by PCR amplification with two different forward primers, specific for the two possible start codons, and a common reverse primer. Amplification with primer pairs including the first ATG codon was undetectable, whereas clear amplification was obtained starting from the second ATG codon. PCR products resolved as several bands of different lengths (Figure 1), and sequencing confirmed that all bands represented different transcripts of the same gene, produced by alternative splicing leading to exon skipping or to exons with different boundaries (Figure 2a). Predicted translation products encoded by the alternative transcripts included proteins truncated at either the amino- or carboxy-terminus as compared to the annotated protein product (Accession # NP_060116, Figure 2b). The same protein fragments could be obtained from translation of several different transcripts, for example, loss of exon 4 in transcripts Tr4, Tr5, Tr6, Tr7, and Tr8 introduced a premature stop signal at the beginning of exon 5 and was associated with a predicted protein product including residues 57–138 (AY702936 – AY702940, Figure 2b). No protein product was predicted for the shortest transcript Tr15 (317 bp) composed only of exons 1 and 11 (AY702947). Only transcript Tr3 might

Figure 1 Reverse contrast image of an ethidium bromide-stained agarose gel showing the RT–PCR results on normal/tumor lung cDNAs; M: size marker φX, 1–12: cDNA samples (N, normal; T, tumor)
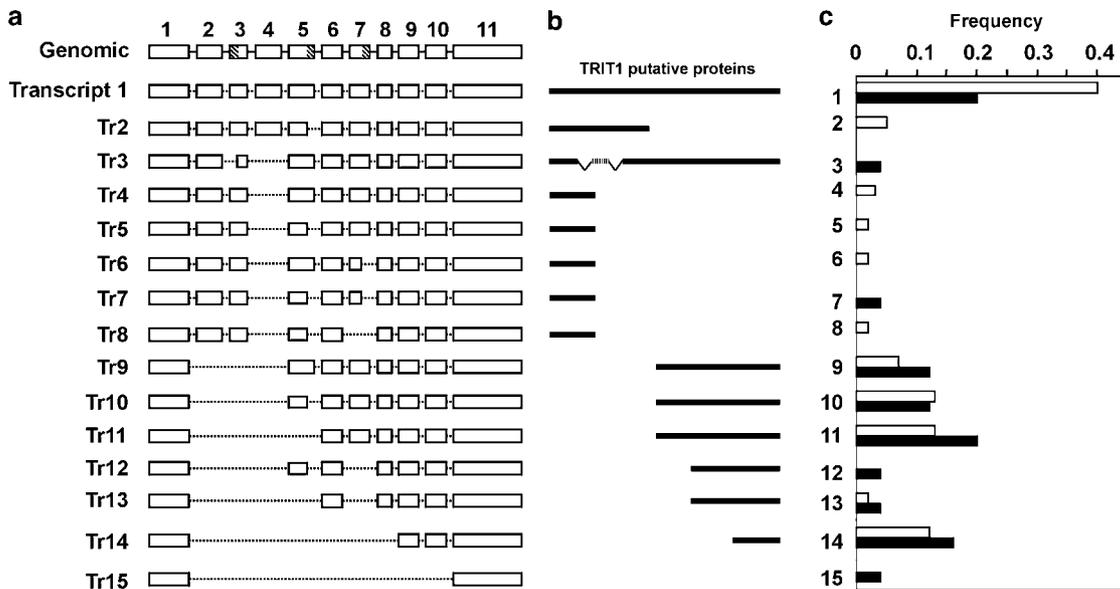
Figure 2 TRIT1 has a complex pattern of alternatively spliced transcripts. (a) Genomic organization of alternatively spliced transcripts and (b) putative corresponding proteins. Open boxes and dotted horizontal lines indicate exons and introns, respectively; hatched areas in exons 3, 5, and 7 indicate sequences that are lost due to alternative splicing. Protein alignments are drawn with respect to the NP_060116 reference protein sequence. (c) Relative frequency of TRIT1 alternative transcripts in normal and tumor lung tissue. White bars, normal lung tissue; black bars, lung cancer

encode a complete protein with a different internal portion: splicing in the junction site between exons 2 and 3 determined a switch to a different frame for 29 amino acids, and the original frame was restored by the successive splicing that skipped exon 4 (AY702935, Figure 2b).

Restoration of tRNA-IPT biochemical activity in yeast

The different transcripts were tested for their functional activity in the yeast strain MT-8, which has defective tRNA-IPT activity and synthesize tRNAs devoid of i⁶A modification, in comparison with yeast strain H57, which produces an active tRNA-IPT gene. Since different transcripts of TRIT1 most likely encode the same protein product, only a subgroup was tested for transformation in yeast: Tr1 (full length, AY702933), Tr3 (complete protein with a partial different sequence, AY702935), Tr2 (longest N-terminal region, AY702934), Tr10 (longest C-terminal region, AY702942), and Tr14 (shortest predicted protein, AY702946).

To determine whether the different transcripts are biochemically active in i⁶A synthesis, tRNAs were extracted, hydrolysed, and analysed, by HPLC and MS. Analysis of tRNAs obtained from control and transformed yeast strains indicated that tRNA-IPT activity was restored only by the lung full-length transcript (Tr1), which displayed functional activity despite the lack of the first 56 amino acids, as compared to the embryo clone (Figure 3a). Deletion of 230 amino
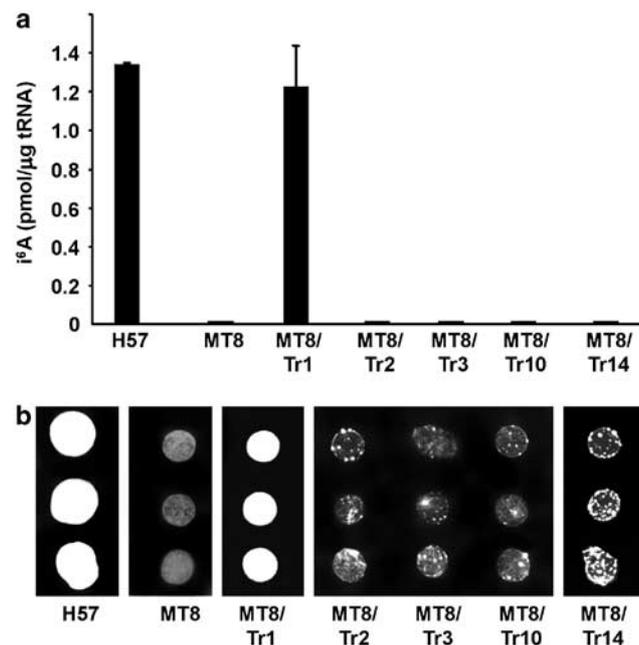
Figure 3 TRIT1 full-length lung transcript restores tRNA-IPT activity in MT-8 yeast strain. (**a**) Determination of i⁶A levels in yeast MT-8 strain transformed with different human TRIT1 transcripts in comparison to wild-type H57 yeast strain. Columns and bars show the mean value and s.e. of 2–3 independent replicas. (**b**) Growth in medium lacking adenine of wild-type H57 yeast strain in comparison to MT-8 strain nontransformed or transformed with different human TRIT1 transcripts

acids in the carboxy-terminal domain or deletion of 191 residues in the amino-terminus abrogated functional activity. Levels of i⁶A produced by the full-length transcripts were similar to that of the control H57 yeast strain (1.22 ± 0.22 and 1.34 ± 0.01 pmol/μg tRNA, respectively). Yeast strains transformed with shorter variants displayed i⁶A amounts below the detection limit, that is, 0.1 pmol/μg tRNA. Transcript Tr3, producing a putative complete protein but with different internal sequences, also revealed no detectable levels of i⁶A (Figure 3a).

Yeast strains devoid of i⁶A modifications are unable to suppress nonsense mutations in *ade2-1* and *lys2-1* alleles and fail to grow on media lacking adenine or lysine. Accordingly, we found that only MT-8 strain expressing Tr1 variant re-acquired adenine and lysine independence, whereas other transcripts gave no functional complementation on selective media (Figure 3b).

Alteration of TRIT1 isoforms expression pattern in lung cancer

Normal and tumor lung tissue were compared for expression of TRIT1 alternative transcripts, which were cloned and identified by nucleotide sequencing. A two-fold under-representation of the full-length transcript (Tr1) was observed in lung tumor tissue as compared to normal lung parenchyma: Tr1 represented 20 and 40% of all sequenced clones, respectively (Figure 2c). The general distribution of the shorter transcripts was slightly higher in cancer than in normal samples, with transcripts Tr9, Tr10, Tr11, and Tr14 being the most frequent in both cases (44 and 60% of total normal and tumor clones, respectively, Figure 2c). Transcripts Tr9, Tr10, and Tr11, which are predicted to encode the same protein product (amino acids 247–467), together represented 33 and 44% of all clones from normal and tumor tissue, respectively (Figure 2c).

TRIT1 expression in normal and tumor lung tissue was further investigated using real-time quantitative PCR (Table 1). Seven different primer pairs were used because of the complex pattern of alternatively spliced transcripts. All primers indicated a reduction in TRIT1 mRNA levels in tumor as compared to normal lung tissue, with values ranging from three- to seven-fold. Comparison of absolute expression levels (ΔC_t values, Table 1) of different exons within the same tissue revealed higher levels for exons 10–11 and 5–6 in both tumor and normal samples, indicating that these exons are included in most of the isoforms, consistent with the molecular cloning results (Figure 2a).

LOH and somatic mutations in lung ADCA

LOH was analysed in 131 paired DNAs from lung tumors and their respective normal tissues; among these pairs, 69 homozygous samples were excluded and LOH was detected in 14 of 62 (23%) informative heterozygous samples. Both alleles were affected indicating no preferential loss. Tumor DNA of the 14 samples showing LOH was further analysed in search

Table 1 Relative TRIT1 gene expression in lung cancer tissue compared to lung normal parenchyma[a]

| Exons	$\triangle C_t$, tumor[b]	$\triangle C_t$, normal[b]	$\triangle \triangle C_t$ ($\triangle C_t$ tumor $-$ $\triangle C_t$ normal)	Fold change ($2^{-\triangle \triangle C_t}$)
1–2	10.15 ± 0.87	8.48 ± 0.64	2.19 ± 0.95	0.22
2–3	9.65 ± 1.85	7.75 ± 1.54	2.38 ± 1.19	0.19
4–5	9.40 ± 1.33	7.03 ± 0.92	2.36 ± 0.42	0.19
5–6	5.60 ± 1.36	4.35 ± 1.75	1.80 ± 0.66	0.29
7–9	10.93 ± 1.31	8.23 ± 1.08	2.71 ± 0.27	0.15
8–9	9.90 ± 1.00	8.00 ± 1.18	1.89 ± 0.56	0.27
10–11	4.40 ± 0.50	2.70 ± 0.59	1.71 ± 0.20	0.31

[a]Mean values $\pm$ s.e. calculated from 3–4 independent replicas in triplicate. Lung normal tissue and lung cancer tissue each represent a pool of 20 samples from separate individuals. [b]$\triangle C_t$ = threshold cycle (C_t), that is, the fractional cycle number at which the amount of amplified target reaches a fixed threshold for TRIT1 minus the C_t for HMBS control

of mutations. Nucleotide sequence analysis of all exons and flanking intronic regions indicated no somatic mutations in lung ADCAs of this group of patients.

Expression of TRIT1 full-length transcript induces morphological changes and inhibits tumorigenesis

A549 human lung carcinoma cells were transfected with the full-length TRIT1 transcript and evaluated *in vitro* for growth characteristics. Real-time quantitative PCR analysis for expression of recombinant vector identified six clones in which TRIT1 mRNA levels were up to 15-fold higher than in nontransfected control cells. These stable transfectant clones and nontransfected cells were plated at the same density and allowed to grow for 12 days; analysis revealed similar numbers of colonies formed in control and transfected cells (158.2 ± 12.7 and 144.3 ± 11.2 colonies, respectively), but the mean area of colonies was 45-fold higher in nontransfected than TRIT1-transfected cells ($P < 0.001$) (Figure 4a and b), with all six transfectant clones producing colonies similarly reduced in size. These results were reproducible with or without selective antibiotic in the medium (not shown). The difference in cell colony size was associated with a change in colony morphology, since nontransfected A549 cells gave flat colonies with higher cell density in the center and spreading cells at the edges (Figure 4b, left top panel), whereas TRIT1-transfected A549 cells produced compact, round colonies, with almost no cell scattering (Figure 4b, right top panel). Cell morphology also differed between the two cell lines, with TRIT1-transfected A549 cells exhibiting a round shape and a reduced cytoplasm (Figure 4b, right bottom panel) as compared to control cells (Figure 4b, left bottom panel).

Groups of 29, 15, and 33 nude mice were injected with nontransfected, Lac-transfected, or TRIT1-transfected (from three independent clones) A549 cells, respectively. Since tumor incidence in mice bearing nontransfected or Lac-transfected cells did not differ significantly (27/29 and 15/15, respectively), these control groups were combined for comparison with TRIT1-transfected cells. A significant difference between the control and TRIT1 groups was observed in tumor incidence: tumors grew in 42/44 (95%) mice injected with control A549 cells and in
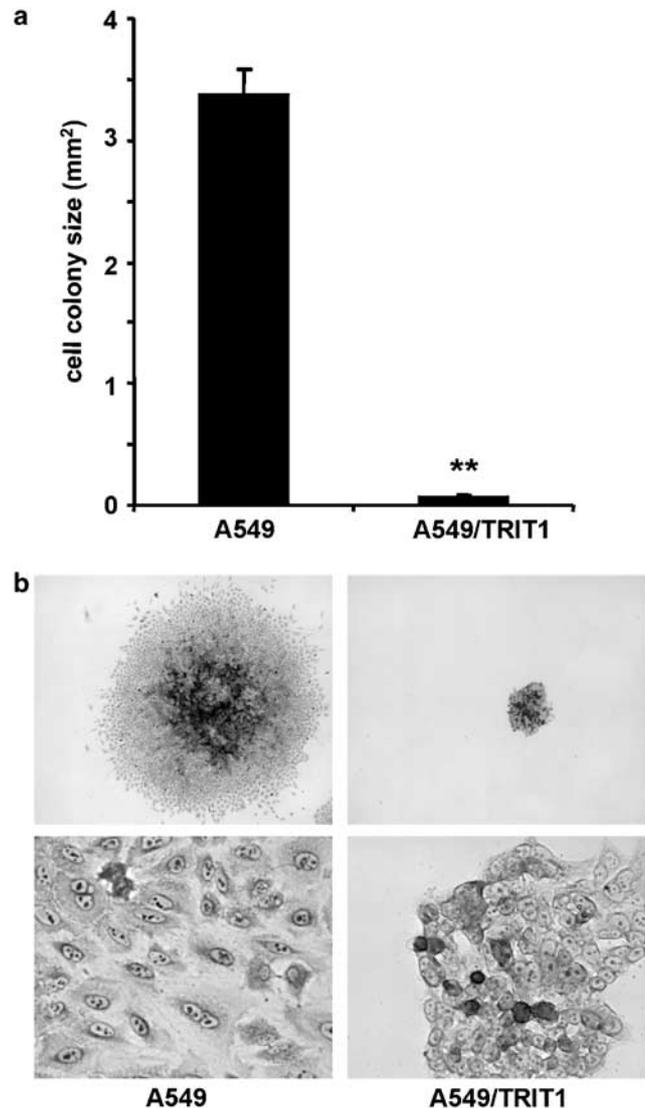
Figure 4 Expression of functional TRIT1 variant affects tumor cells growth *in vitro* and *in vivo*. (**a**) *In vitro* cell colony formation assay of nontransfected ($n = 5$) and TRIT1 stable transfectant ($n = 17$) A549 human lung cancer cells. ** $\sim$45-fold smaller colony area, $P < 0.0001$. (**b**, top) Decreased colony size in TRIT1-transfected A549 cells (right) as compared to nontransfected cells (left). (**b**, bottom) Nontransfected cells displayed a large cytoplasm, grew flat and scattered (left), whereas TRIT1-transfected cells displayed a small cytoplasm and grew tightly joined with a sharp demarcation of the colony border (right)
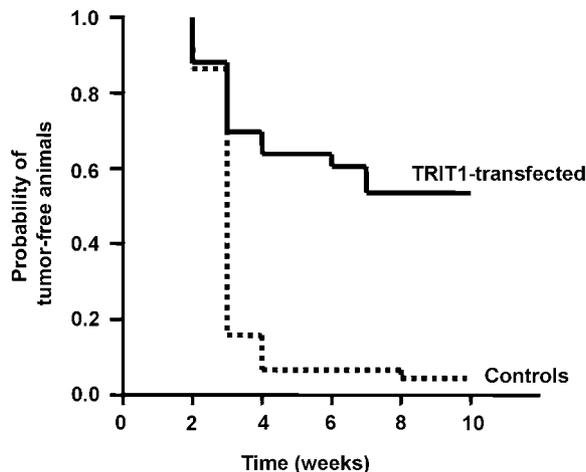
Figure 5 Kaplan–Meier curves showing time-dependent decreased tumor incidence in nude mice injected with TRIT1-transfected (three clones, 33 mice) as compared to 44 mice injected control A549 cells ($P<0.0001$, log-rank)

15/33 (45%) mice injected with TRIT1-transfected cells ($P<0.0001$, Figure 5).

Discussion

Analysis of TRIT1 gene expression in lung tissue revealed a full-length transcript that skips the first ATG start codon present in the mRNA cloned from embryo, with another putative methionine corresponding to amino acid 57 of the reported sequence. Previous analysis of conserved motifs in the reported human TRIT1 transcript identified an ATP/GTP motif A in the amino-terminal portion of the protein (residues 30–37) (Golovko *et al*., 2000). Although neither ATP nor GTP is a direct substrate of tRNA-IPT enzymes, an inhibitory effect of several di- and tri-nucleotides has been described in both *E. coli* (Leung *et al*., 1997) and *A. thaliana* (Sakakibara and Takei, 2002), thus pointing to a possible regulatory role of this domain for the enzymatic activity *in vivo*. However, the full-length lung TRIT1 transcript lacking the amino-terminal domain almost completely complemented the yeast tRNA-IPT biochemical activity, resulting in the production of amounts of i⁶A-tRNA similar to those produced by the wild-type yeast *MOD5* gene, when introduced into a yeast mutant strain with defective tRNA-IPT activity. In lung tissue, the TRIT1 gene showed a complex pattern of alternatively spliced variants differing in the presence/absence of entire exons or in different exon boundaries and representing a significant percentage of all mRNA transcripts.

Alternative splicing has an important role in expanding protein diversity and it is now well established that many human genes are alternatively spliced. The presence of alternative splicing in many organisms raises intriguing questions on its functions and the involvement in regulation of essential biological processes. As

for the TRIT1 gene, functional complementation experiments in yeast indicated that only the full-length isoform is biochemically active and it is not clear whether the other transcripts produce short TRIT1-like proteins, especially the Tr9–Tr14 transcripts whose putative ATG start codon is localized in exon 6 and would encode a product containing only the C-terminal region of the complete TRIT1 protein (AY702941–AY702946). Moreover, one full-length transcript (Tr3) with a different internal amino acid sequence (Figure 2b, AY702935) was not functional (Figure 3a and b), indicating that maintenance of the correct sequence of the whole IPT domain (residues 57–346) is essential for enzyme activity.

We showed that TRIT1 variants are expressed in both normal and tumor lung tissues. Overall, endogenous expression of the TRIT1 gene was 3–7-fold down-regulated in human lung adenocarcinoma samples as compared to normal lung tissue. Moreover, the relative abundance of the functional full-length transcript was more affected than that of other mRNA variants, and resulted to be about 50% lower in human lung adenocarcinoma than in normal lung tissue. Together, these data indicate that levels of the functional TRIT1 transcript are 6–14-fold decreased in lung cancer as compared to the normal lung tissue. Reduction of TRIT1 expression in human lung tumors can be partially explained by LOH that we detected in about 23% of lung cancer patients. However, alternative mechanisms might be involved, such as silencing of control regions by methylation or alteration of trans-acting repressors or activators of the TRIT1 gene.

TRIT1 was transfected in A549 human lung carcinoma cell line, whose endogenous TRIT1 levels were ~20-fold lower than those measured in human normal lung tissue (not shown). Expression of the functional mRNA isoform in A549 cells caused morphological alteration and inhibition of colony-forming efficiency, resulting in colonies of significantly smaller size as compared to parental cancer cells (Figure 4a and b). Furthermore, stable TRIT1-transfected A549 cells showed a reduced tumorigenicity in nude mice (Figure 5). These results suggest a functional role of the human TRIT1 gene in the negative control of tumorigenesis.

Post-transcriptional modifications of tRNAs are known to be important in assuring correct protein synthesis, and effects of tRNA-IPT on translation have been demonstrated in yeast. Indeed, strains devoid of this enzymatic activity lack i⁶A modification of the nuclear-encoded tRNA SUP7 molecule, which consequently cannot act as a nonsense suppressor (Gillman *et al*., 1991). Our findings indicate that the human TRIT1 gene maintains the nonsense suppressor activity and can play an essential role in protein translation. In mammals, i⁶A is found in selenocysteine (Sec) tRNA (tRNA[Ser]Sec) that decodes UGA stop codons and inserts Sec residues into nascent peptides. The ability to decode UGA as a Sec codon requires specific mRNA secondary structures and specific translational factors (Low and Berry, 1996; Berry *et al*., 2001) and is affected when tRNA[Ser]Sec lacks i⁶A at position 37, as demonstrated by

studies in *Xenopus* (Warner *et al.*, 2000). Similarly, transgenic mice overexpressing i[6]A-deficient tRNA[Ser]Sec show defective levels of numerous selenoproteins due to problems occurring during translation and not transcription since mRNA levels remain unchanged (Moustafa *et al.*, 2001).

Many studies have correlated deregulation of protein biosynthesis with cancer, but it remains to be ascertained whether this process is necessary and/or sufficient for neoplastic transformation. Our results provide evidence that a gene affecting translation can show LOH and alteration of mRNA expression in lung cancer, and that expression of the functional gene in cancer cells partially suppresses the tumor phenotype. This effect might be achieved by regulation of efficiency and fidelity of the protein synthesis machinery, thus supporting the idea that genes controlling mRNA translation, although indirectly, may have an important role in cancer.

Materials and methods

Tissue samples

Specimens of human normal lung parenchyma and lung adenocarcinoma tissue (histopathologically confirmed) were obtained from surgical resection of lung cancer patients at Istituto Nazionale Tumori (Milan, Italy). Total RNA was extracted from 20 samples of normal lung tissue and 20 samples of lung tumor tissue with RNeasy Midi kit (Qiagen, Valencia, CA, USA). Equal amounts of lung normal RNAs and lung tumor RNAs were pooled, respectively, and the two RNA pools were reverse-transcribed using the SuperScript™ First-Strand Synthesis System (Invitrogen, Carlsbad, CA, USA).

Screening of a human lung cDNA library

A human lung cDNA library 'RAPID-SCREEN cDNA LIBRARY PANELS' (OriGene Technologies Inc., Rockville, MD, USA) was screened using forward primer 5′-caacggaccc-tacctcttgt-3′ and reverse primer 5′-ctctgctcttgggcagaaac-3′ following the manufacturer's instructions. Screening of the whole plate revealed 17 possible positive clones, nine of which were confirmed in an independent subsequent PCR reaction. Positive clones were PCR-amplified using vector-specific forward primer (5′-gtaatacgactcactatagggc-3′) and gene-specific reverse primer. PCR products were purified by QIAquick PCR purification kit (Qiagen, Valencia, CA, USA) and sequenced on an ABI-PRISM 377 automatic sequencer (Applied Biosystems, Foster City, CA, USA).

Cloning of alternatively spliced transcripts

Two forward primers (5′-actgccataagatggcgtc-3′ and 5′-caacg-gaccctacctcttgt-3′ starting at nucleotide 4 and 72 of sequence NM_017646, respectively) and a common reverse primer (5′-caccttteccaaaggccact-3′ at nucleotide 1448) were designed for amplification of the human TRIT1 gene. PCR reactions were carried out in a 50-μl volume containing aliquots of normal lung cDNA, 80 μM dNTPs, 10 pmol of each primer pair, 1.5 mM MgCl$_2$, buffer 1×, 2.5 U BIO-X-ACT DNA polymerase (Bioline). A total of 40 PCR cycles were performed (95°C × 30 s, 57°C × 20 s, 72°C × 90 s) in a GeneAmp PCR system 9700 machine (Applied Biosystems). Aliquots of 5 μl of PCR products were loaded on 2% agarose gels and stained with ethidium bromide.

PCR amplification of the alternatively spliced transcripts was carried out in 50 μl containing 200 μM dNTPs, 10 pmol of gene-specific PCR primers, 2.5 mM MgCl$_2$, buffer 1×, 2.5 U BIO-X-ACT DNA polymerase (Bioline) for 40 PCR cycles (95°C × 30 s, 57°C × 30 s, 72°C × 2 min) in a GeneAmp PCR system 9700 machine (Applied Biosystems). Aliquots (10 μl) of PCR products were loaded on 2% agarose gels and stained with ethidium bromide. PCR products were cloned in cloning vector pCR2.1/V5-His-TOPO (Invitrogen, Carlsbad, CA, USA) and sequenced.

Real-time quantitative PCR

Gene-specific primers were designed to be intron-spanning (Table 2). Specificity of PCR primers was checked by agarose gel analysis of the PCR products and by melting curve analysis of the amplicons. Primers were used for quantitative analyses only if primer dimers and unspecific products were not detected. Real-time PCR amplification mixtures contained 0.5 μl of template cDNA pooled from normal or tumor lung tissue, 12.5 μl 2× QuantiTect SYBRGreen PCR Master Mix (Qiagen, Valencia, CA, USA), and 0.3 μM specific PCR primers. Final volume was adjusted to 25 μl. Reactions were run in triplicate on an ABI GeneAmp 5700 sequence detection system (Applied Biosystems) for 40 cycles (94°C for 15 s/60°C for 10 s/72°C for 20 s) after an initial activation step at 95°C for 15 min. The human hydroxymethylbilane synthase (HMBS) gene (GenBank Acc. #) (NM_000190) was used as a housekeeping control for possible differences in cDNA amounts. Relative differences (-fold) were calculated according to the comparative C_t method using the normal lung cDNA pool as calibrator.

Table 2 PCR primers used for real-time quantitative PCR

Gene	Exons	Forward primer	Reverse primer	PCR product length (bp)
TRIT1	1–2	CAACGGACCCTACCTCTTGT	CTCTGCTCTTGGGCAGAAAC	170
	2–3	ATGCAGGTCTATGAAGGCCT	AATTGGTTCCTCCCACAACA	202
	3–4	CATTGAATCTCTGCTCTGGAAA	TCCTCCTTTTCAAGCTCCAC	100
	4–5	ATGGGCACTGAGAAAGTGAT	CCTTCTTCCGTATGTTGACGA	209
	5–6	TACGGAAGAAGGTGGTGGTC	CCTCTTATCCAAGCGCTCAT	109
	7–9	AGGGAAAATGCACACTGGAG	TTGCACGATTTCAAGAGCAG	222
	8–9	GAGATATGCCCGGAAACAAA	TTGCACGATTTCAAGAGCAG	149
	10–11	TGTGTGACCTCTGTGATCGAA	GGTCTGGGGAAACACTCTGA	150
HMBS		AGGATGGGCAACTGTACCTG	GCCTACCAACTGTGGGTCAT	137

LOH and somatic mutations analyses

Single-nucleotide polymorphism rs6680378 located in intron 1 of TRIT1 gene was used for LOH analysis. Paired genomic DNAs were extracted with the automatic DNA extractor Extragen 8C (Talent, Trieste, Italy) from surgically resected normal and tumor tissue of Italian lung adenocarcinoma patients. DNA samples were amplified by PCR with forward primer gcctcagctcatttcctagc and 5′-biotinilated reverse primer ccccacaacaaccctatgag to allow analysis by pyrosequencing. PCR reactions were run in 27 μl containing 50 ng of genomic DNA, 100 μM dNTPs, 7.5 pmol of each primer, 0.5 U Amplitaq Gold DNA polymerase (Applied Biosystems) for 40 cycles (95°C × 15 s, 57°C × 10 s, 72°C × 20 s) in a GeneAmp PCR system 9700 machine (Applied Biosystems). Quality of PCR amplifications was checked by loading 4 μl of the reaction products on ethidium bromide-stained 3% agarose gel. Samples were automatically genotyped by pyrosequencing on a PSQ96MA system (Biotage AB, Uppsala, Sweden) with primer ctctctgggcctcaatc according to the manufacturer's instructions. Allele frequencies of the two alleles were calculated in three replicas of normal and tumor tissue of heterozygous samples. Experiment was carried out in duplicate to confirm the observed results. A difference of 30% or more in allele frequency in tumor DNA as compared to normal DNA was considered evidence for LOH.

Lung tumor DNA of samples showing LOH was sequenced to search for somatic mutations. All exons of TRIT1 were PCR amplified with specific primers mapping on flanking intronic regions (exon 1: ggggttcacccttttaagacc, aacctcgcta caaagcctga; exon 2: ccatagtctgatgggggatgg, cagtgaagtgtttggcag ga; exon 3: cagcaagaaagagcaatcca, ttgctaatggtgtccttcca; exon 4: ataactcagggcctcccaac, agggaagcaaatagccaggt; exon 5: atgc cagggctatcctttct, ctgtcgtgactggctttcaa; exon 6: aaactgcatctg caaagaagg, aggaggcatgtgcttcattc; exons 7 and 8: cagacccataggataaa gaaaaaca, ctgctcaggatctcaatttcc; exon 9: agccagcccttctgctttta, gatcctgcacccatgtatcc; exon 10: cctccaaggaatttgagcac, agggct ggctgctttttaat; exon 11: acacatcagccacacaagga, cccttaaaaatgc taagcagcta). PCR reactions were run in 25 μl containing 30 ng of genomic DNA, 80 μM dNTPs, 5 pmol of each primer, 0.5 U Amplitaq Gold DNA polymerase (Applied Biosystems) for 40 cycles (95°C × 30 s, 57°C × 20 s, 72°C × 30 s) in a GeneAmp PCR system 9700 machine (Applied Biosystems). Quality of PCR amplifications was checked by loading 3 μl of the reaction products on ethidium bromide-stained 2% agarose gel. Samples were sequenced at BMR-CRIBI (University of Padua, Italy).

Yeast transformation and functional screening of TRIT1 transcripts

Selected alternatively spliced transcripts were cloned in the yeast expression vector pYES2.1/V5-His-TOPO (Invitrogen). Transformant colonies were sequenced and clones with no mutations were chosen to transform *S. cerevisiae* strains MT-8 (*MATα SUP7 ura3-1 his5-2 leu2-3,112 ade2-1 trp1 lys1-1 can1-100 mod5::TRP1*) and H57 (*MATα MOD5 SUP7 can1-100 ade2-1 his5-2 lys1-1 ura3-1*). Yeast strains were maintained on YPD medium or synthetic complete medium lacking appropriate nutrients to select for the presence of plasmid. Yeast cells were transformed using the LiOAc method (Gietz and Schiestl, 1997).

Analysis of i⁶A by ESI LC-MS-MS

Yeast cells were grown to mid-log phase and harvested. tRNA was extracted using NucleobondAX (Macherey-Nagel), fol-lowing the manufacturer's instructions, eluted with 100 mM Tris/acetate, 15% ethanol, pH 6.3, and 0.6 M KCl, and digested (12 μg) with nuclease P1 (Roche) followed by bacterial alkaline phosphatase (Sigma) (Gehrke *et al.*, 1982). After hydrolysis, samples were mixed with N^6-(3-[1,1,1-$^2H_3$]methyl-[4,4,4-$^2H_3$]-but-2-enyl)adenosine ($^2H_6$-i⁶A) (OlChemIm Ltd., Olomouc, Czech Republic) used as internal standard for LC-MS/MS analysis (50 μl, 95 pmol) and a 10-μl aliquot was injected into the HPLC column.

i⁶A was quantitated using a SpectraSYSTEM P400 HPLC connected to a LCQ-Deca® (ThermoQuest, San Jose, CA, USA) ion trap mass spectrometer equipped with an electrospry ionization source (ESI). The HPLC and MS systems were run using Xcalibur 1.2 software (ThermoQuest). A Nucleosil 100 C8 column (5-μm, 15 × 0.21 cm; Teknokroma, Barcelona, Spain) was used for chromatographic separations. The mobile phase consisted of 5 mM ammonium acetate (pH = 6.0) (A) and methanol (B). Gradient elution at a flow rate of 0.2 ml/min for a total of 15 min was as follows: 55% B for 6 min, linear to 100% B in 1 min, 100% B for 2 min, linear to 55% B for 1 min followed by 5 min equilibration before the next injection. The conditions of the ESI source were: capillary temperature 220°C, sheath gas (nitrogen) flow rate at 60 U, auxiliary gas 10 U, spry voltage 5.0 kV. Capillary voltage was set at 43 V in positive ion ionization mode. Relative collision energy was set at 35% for each compound, isolation width was fixed at 2.0 and product ions were scanned. The amount of i⁶A in the samples was estimated from a standard curve obtained by adding increasing amounts of i⁶A (5.3–426 pmol) to a fixed amount of $^2H_6$-i⁶A (95 pmol) to cover the ratio range of I⁶A/$^2H_6$-i⁶A at 0.055–4.48.

In vitro *functional assays*

TRIT1 full-length transcript was cloned in pCR3.1/V5-His-TOPO (Invitrogen) for transfection into the A549 (CCL-185) human lung carcinoma cell line. Cells were transfected with 2.5 μg DNA of recombinant or control vector (pCR3.1/V5-His-TOPO/*lacZ*) using SuperFect Transfection Reagent (Qiagen, Valencia, CA, USA). Transfected clones were grown in selective medium containing 1 mg/ml geneticin (G-418 sulfate) (Invitrogen) for 3 weeks. Total RNA was extracted from transfectant clones with RNAfast-II Isolation Kit (Molecular Systems, San Diego, CA, USA) and reverse-transcribed with SuperScript™ First-Strand Synthesis System (Invitrogen). Expression of recombinant vectors was checked by real-time quantitative PCR (see above), using gene-specific primers 5′-cttgtagtgattcctcggggc-3′ and 5′-ctctgctcttgggcagaaac-3′. The HMBS gene served as a control for differences among samples in cDNA quantities, and RNA from nontransfected cells was used as calibrator.

For each plate, 1000 cells of six independent stable transfectant clones and nontransfected A549 cells were plated (2–5 plates/clone), grown for 12 days, methanol-fixed, and stained with 10% Giemsa. Experiments were performed both with and without selective antibiotic in the medium. Scanned images of plates were analysed with Quantity One software (Bio-Rad) for cell counts. Colony diameters were measured microscopically.

In vivo *assay*

Groups of 15–33 nude mice were injected subcutaneously (s.c.) into the right dorsal region with 3×10^6 A549 cells transfected with TRIT1 (three independent stable transfectant clones), Lac-vector, or left nontransfected. Tumor size was measured weekly by a Vernier caliper. The experiment was terminated at

10 weeks after injection, when representative tumors were excised, fixed in buffered formalin, embedded in paraffin, cut into sections, and stained with hematoxylin and eosin.

Statistical analysis

Cell colony size was analysed using ANOVA. The Kaplan–Meier product-limit method and the log-rank test were used to estimate time-dependent tumor incidence curves in nude mice.

Both statistical tests were carried out using the SPSS 10.1 software (SPSS Inc., Chicago, IL, USA).

References

Berry MJ, Tujebajeva RM, Copeland PR, Xu XM, Carlson BA, Martin GW, III, Low SC, Mansell JB, Grundner-Culemann E, Harney JW, Driscoll DM and Hatfield DL. (2001). *Biofactors*, **14,** 17–24.

Bjork GR, Durand JM, Hagervall TG, Leipuviene R, Lundgren HK, Nilsson K, Chen P, Qian Q and Urbonavicius J. (1999). *FEBS Lett.*, **452,** 47–51.

Bjornsti MA and Houghton PJ. (2004). *Cancer Cell*, **5,** 519–523.

Caillet J and Droogmans L. (1988). *J. Bacteriol.*, **170,** 4147–4152.

Connolly DM and Winkler ME. (1989). *J. Bacteriol.*, **171,** 3233–3246.

Diaz I, Pedersen S and Kurland CG. (1987). *Mol. Gen. Genet.*, **208,** 373–376.

Dihanich ME, Najarian D, Clark R, Gillman EC, Martin NC and Hopper AK. (1987). *Mol. Cell. Biol.*, **7,** 177–184.

Dirheimer G, Baranowski W and Keith G. (1995). *Biochimie*, **77,** 99–103.

Gehrke CW, Kuo KC, McCune RA, Gerhardt KO and Agris PF. (1982). *J. Chromatogr.*, **230,** 297–308.

Gietz RD and Schiestl RH. (1997). *Methods Mol. Cell. Biol.*, **5,** 255–269.

Gillman EC, Slusher LB, Martin NC and Hopper AK. (1991). *Mol. Cell. Biol.*, **11,** 2382–2390.

Golovko A, Hjalm G, Sitbon F and Nicander B. (2000). *Gene*, **258,** 85–93.

Lemieux J, Lakowski B, Webb A, Meng Y, Ubach A, Bussiere F, Barnes T and Hekimi S. (2001). *Genetics*, **159,** 147–157.

Leung HC, Chen Y and Winkler ME. (1997). *J. Biol. Chem.*, **272,** 13073–13083.

Low SC and Berry MJ. (1996). *Trends Biochem. Sci.*, **21,** 203–208.

Miller CO, Skoog F, von Saltza MH and Strong F. (1955). *J. Am. Chem. Soc.*, **77,** 1392–1393.

Mok MC. (1994) Mok DWS and Mok MC (eds). *Cytokinins. Chemistry Activity, and Function*. CRC Press: Boca Raton, pp 155–166.

Moustafa ME, Carlson BA, El Saadani MA, Kryukov GV, Sun QA, Harney JW, Hill KE, Combs GF, Feigenbaum L, Mansur DB, Burk RF, Berry MJ, Diamond AM, Lee BJ, Gladyshev VN and Hatfield DL. (2001). *Mol. Cell. Biol.*, **21,** 3840–3852.

Persson BC. (1993). *Mol. Microbiol.*, **8,** 1011–1016.

Persson BC, Esberg B, Olafsson O and Bjork GR. (1994). *Biochimie*, **76,** 1152–1160.

Rozenski J, Crain PF and McCloskey JA. (1999). *Nucleic Acids Res.*, **27,** 196–197.

Sakakibara H and Takei K. (2002). *J. Plant Growth Regul.*, **21,** 17–23.

Takei K, Sakakibara H and Sugiyama T. (2001). *J. Biol. Chem.*, **276,** 26405–26410.

Urbonavicius J, Qian Q, Durand JM, Hagervall TG and Bjork GR. (2001). *EMBO J.*, **20,** 4863–4873.

Warner GJ, Berry MJ, Moustafa ME, Carlson BA, Hatfield DL and Faust JR. (2000). *J. Biol. Chem.*, **275,** 28110–28119.